

# Electronic and optical properties of $2H$ -WSe<sub>2</sub> intercalated with copper

Ali Hussain Reshak and S. Auluck

*Physics Department, Indian Institute of Technology, Roorkee (Uttaranchal) 247667, India*

(Received 25 November 2002; published 10 November 2003)

We have studied the electronic properties of  $2H$ -WSe<sub>2</sub> intercalated with Cu using the full-potential linear-augmented plane-wave method as implemented in the WIEN97 code. Intercalating  $2H$ -WSe<sub>2</sub> with Cu changes the electronic behavior from semiconducting to metallic. We present calculations of Cu<sub>*x*</sub>WSe<sub>2</sub> for  $x=0.5$  and  $1.0$ . The copper-*d* partial density of states in Cu<sub>*x*</sub>WSe<sub>2</sub> is similar to that in pure copper. As in the case of copper, the Cu *d* bands are flat and lie 2–4 eV below  $E_F$ . Our calculations show that there is weak hybridization between the Cu states and W and Se states. We have also calculated the frequency-dependent dielectric properties of Cu<sub>*x*</sub>WSe<sub>2</sub> with a view to ascertain the effect of copper intercalation on the optical properties.

DOI: 10.1103/PhysRevB.68.195107

PACS number(s): 71.15.-m

## I. INTRODUCTION

During recent years, transition-metal dichalcogenides of groups IVB, VB, and VIB have received considerable attention because of the great diversity in their physical properties.<sup>1,2</sup>  $2H$ -WSe<sub>2</sub>, an interesting member of the transition-metal dichalcogenide compound (TMDC) family, is known to be a semiconductor with a measured indirect gap of 1.2 eV, thus making it useful for photovoltaic and optoelectronic applications.<sup>3</sup> Electrochemical devices based on  $2H$ -WSe<sub>2</sub> have been reported to possess conversion efficiencies up to 17% (Ref. 4).  $2H$ -WSe<sub>2</sub> and its intercalation compounds are known for their remarkable stability against photocorrosion.<sup>5,6</sup>  $2H$ -WSe<sub>2</sub> has recently been a subject of a number of photoemission studies.<sup>7–10</sup> In general, good agreement is found between theory and experiment, thereby lending support to calculational techniques based on the density functional theory (DFT) using the local density approximation (LDA) as well as the experimental techniques of the angular-resolved and inverse angular-resolved photoemission spectroscopy.

There exist a number of calculations of the electronic structure of  $2H$ -WSe<sub>2</sub>. Coehoorn *et al.*<sup>7</sup> used the augmented spherical-wave (ASW) method. The valence-band maxima (VBM) was located at  $\Gamma$  and the conduction-band minima (CBM) about midway in the  $\Gamma K$  direction, resulting in an indirect gap of 0.35 eV. Traving *et al.*<sup>10</sup> reported band calculations based on the fully relativistic linear muffin-tin orbital (RLMTO) and extended linear-augmented plane-wave (ELPAW) methods. The RLMTO calculations put the VBM at  $K$  (the highest valence band at  $\Gamma$  is only 18 meV below the Fermi energy), and the CBM is also at  $K$ , giving a direct band gap of 0.4 eV. Straub *et al.*<sup>8</sup> and Finites *et al.*<sup>9</sup> reported a full potential linear augmented plane-wave (FPLAPW) calculation and showed that the VBM is located at the sixfold-degenerate point  $K$  while the CBM lies midway along the  $\Gamma K$  direction. This finding was supported by their own photoemission data. An energy gap of 0.8 eV was found. A correction<sup>9</sup> places the VBM at  $\Gamma$  at variance with their own experimental data, but in agreement with other theoretical calculations. Sharma *et al.*<sup>11</sup> calculated the frequency-dependent anisotropic dielectric function  $\epsilon^\perp(\omega)$  and  $\epsilon^\parallel(\omega)$  corresponding to the electric field perpendicular and parallel

to the *c* axis and compared their results with the experimental data.<sup>12–15</sup>

Interest in copper-intercalated TMDC has recently been picking up. Kusawake *et al.*<sup>16–18</sup> have reported measurements of the diffuse x-ray intensity on the local arrangements of intercalated copper atoms in the layered Cu<sub>*x*</sub>TiS<sub>2</sub> compounds with  $x$  varying from 0.13 to 0.37. Two kinds of diffuse scattering, corresponding to  $2 \times 2$  and  $\sqrt{3} \times \sqrt{3} R30^\circ$  structures, are observed. They found that while the lattice constant (**a**) remains the same, the lattice constant (**c**) varies with concentration  $x$  increasing by 3% at  $x=0.61$ . Using x-ray structure analysis and the electron density distribution, they found that Cu atoms occupy the tetrahedral sites. They reported different positions of the Cu atoms in the hexagonal lattice depending on the concentration. A new spinal phase for Cu<sub>*x*</sub>TiS<sub>2</sub> is also reported. Klein *et al.*<sup>19</sup> have reported a photoemission study of barrier and transport properties of interfaces of Au and Cu on a  $2H$ -WSe<sub>2</sub> (0001) surface. Patel *et al.*<sup>20</sup> have studied the intercalation of copper with  $2H$ -WSe<sub>2</sub> using direct vapor transport techniques. From the x-ray diffractogram, the lattice parameter and x-ray density for Cu<sub>*x*</sub>WSe<sub>2</sub> is obtained. They show that intercalating  $2H$ -WSe<sub>2</sub> with copper makes it conducting and the conductivity increases with the copper concentration.

It is clear that even though some experimental work has been done on the intercalated  $2H$ -WSe<sub>2</sub>, theoretical work in this direction is almost nonexistent. We believe that our calculation will, at least, start to fill this gap. As we have studied  $2H$ -WSe<sub>2</sub> earlier,<sup>11</sup> a natural extension would be to study the effect of intercalating  $2H$ -WSe<sub>2</sub> with Cu. In particular, our calculations could throw light on the effect of intercalation on band structure, density of states, and optical properties. In this paper we report calculations for the Cu<sub>*x*</sub>WSe<sub>2</sub> compounds for  $x=0.5$  and  $1$ . We compare our results with  $2H$ -WSe<sub>2</sub> to ascertain the effect of copper intercalation on the electronic and optical properties.

In Sec. II we give details of our calculations. The band structure and density of states are presented and discussed in Sec. III. The frequency-dependent dielectric properties are given in Sec. IV, and Sec. V summarizes our conclusions.

## II. DETAILS OF CALCULATIONS

We have performed calculations using the FPLAPW method in a scalar relativistic version as incorporated in the

TABLE I. Experimental lattice parameters of  $\text{Cu}_x\text{WSe}_2$  for ( $x=0, 0.5$ , and  $1.0$ ).

	$\text{WSe}_2$	$\text{Cu}_{1/2}\text{WSe}_2$	$\text{CuWSe}_2$
<b>a</b> (in Å)	3.282 <sup>a</sup>	3.2818 <sup>b</sup>	3.2818 <sup>b</sup>
<b>c</b> (in Å)	13.459 <sup>a</sup>	13.0564 <sup>b</sup>	13.0868 <sup>b</sup>
<b>z</b>	0.621 <sup>a</sup>	0.623 <sup>c</sup>	0.622 <sup>c</sup>

<sup>a</sup>References 16, 10.<sup>b</sup>Reference 21.<sup>c</sup>Optimized.

WIEN97 code.<sup>21</sup> We find from our previous work<sup>11</sup> on  $\text{WSe}_2$  that the spin-orbit interaction has a minor influence on the optical properties. Hence we choose to neglect it in this work.  $\text{WSe}_2$  crystallizes in the  $2H$  phase [space group  $P6_3/mmc$  ( $D_{6h}^4$ )], the two W atoms are located at  $2c$  sites  $\pm(1/3, 2/3, 1/4)$  and the four Se atoms at  $4f$  sites  $\pm(1/3, 2/3, \mathbf{z})$ ,  $\pm(2/3, 1/3, \mathbf{z}-1/2)$ . As there are no crystallographic data for  $\text{Cu}_x\text{WSe}_2$ , we have taken the same crystal structure as  $2H\text{-WSe}_2$ . We have placed the Cu atom at one  $2a$  site for  $\text{Cu}_{1/2}\text{WSe}_2$  and both  $2a$  sites  $(0,0,0)$  and  $(0,0,0.5)$  for  $\text{CuWSe}_2$ . We have taken this cue from Coehoorn *et al.*<sup>7</sup> and Traving *et al.*<sup>10</sup> who placed two empty spheres at the  $2a$  sites to increase the packing fraction. Calculations are performed at the experimental<sup>20</sup> values of the lattice constants **a** and **c**. As can be seen from the atomic positions above, there is only one free structural parameter **z** (also called the internal parameter) that needs to be determined to obtain the complete structural data. The experimental value of **z** for  $2H\text{-WSe}_2$  is 0.621 (Ref. 11), but no experimental values are available for Cu-intercalated  $2H\text{-WSe}_2$ . We have calculated the total energies for various values of **z** and taken the optimized **z** value to be the one corresponding to the minimum total energy. We obtain  $\mathbf{z}=0.623$  and  $0.622$  for the Cu-intercalated  $2H\text{-WSe}_2$  compounds. These values are close to the experimental value of 0.621 for  $2H\text{-WSe}_2$  and all are very close to the ideal value of  $5/8$ . In Table I we collect all the structural parameters used in our work. Self-consistency was obtained using 200  $k$  points in the irreducible Brillouin zone (IBZ), and the BZ integration was carried out using the tetrahedron method.<sup>22,23</sup> The density of states and optical properties are calculated using 450  $k$  points in the IBZ, using the code developed by Ambrosch-Draxl *et al.*<sup>24</sup>

### III. RESULTS AND DISCUSSIONS

#### A. Band structure

Let us recall the main features of the band structure of  $2H\text{-WSe}_2$  (Ref. 11). The VBM is at  $\Gamma$  and the CBM is half way between  $\Gamma K$ , resulting in an indirect gap of 1.2 eV. The band structure can be divided into three main groups. The lowest four bands are mainly Se  $s$  states, the bands between  $-7$  and  $0$  eV, and the bands between  $1$  and  $8$  eV have significant contribution from W  $d$  and Se  $p$ . The bands in the higher-energy range have contributions from W  $s$ , Se  $p$ , and Se  $d$  states.

Figure 1(a) shows the band structure of  $\text{Cu}_{1/2}\text{WSe}_2$ . The conduction and valence bands are shifted towards lower en-

ergy by  $1\text{--}1.5$  eV with respect to  $E_F$  compared to  $2H\text{-WSe}_2$ . Once again, we see three distinct groups of bands (although more broadened) as in  $2H\text{-WSe}_2$ . As a result of intercalation, there is an increase in the number of flat bands just below  $E_F$ , which may be attributed to the Cu  $d$  states. Only one band cuts  $E_F$  in the directions  $\Gamma M$ ,  $MK$ , and  $K\Gamma$ , thus making  $\text{Cu}_{1/2}\text{WSe}_2$  metallic. The increase in the number of bands (compared to  $2H\text{-WSe}_2$ ) above the  $E_F$  is due to the downward shift of the bands relative to  $E_F$ .

In Fig. 1(b) we show the band structure of  $\text{CuWSe}_2$ . The conduction and valence bands are shifted towards the lower energy (with reference to the Fermi energy) by further 1 eV compared to  $\text{Cu}_{1/2}\text{WSe}_2$ . As a result of intercalating more copper, there is an increase in the number of flat bands just below  $E_F$ , compared to  $\text{Cu}_{1/2}\text{WSe}_2$ . The copper  $d$  bands lie  $2\text{--}4$  eV below  $E_F$  in both copper-intercalated compounds.  $\text{CuWSe}_2$  is also metallic, with two bands now cutting  $E_F$ . The bands cutting  $E_F$  have mainly W  $d$  and Se  $p$  character with a small amount of Cu  $s$  character. We observe that the second and third group of bands are more closer to each other in  $\text{Cu}_{1/2}\text{WSe}_2$  (compared to  $2H\text{-WSe}_2$ ) and almost overlap in  $\text{CuWSe}_2$ . One major difference between the band structure of  $\text{Cu}_{1/2}\text{WSe}_2$  and  $\text{CuWSe}_2$  and  $2H\text{-WSe}_2$  is the splitting of the Se  $s$  states (more prominent in the  $MK$  direction). In  $2H\text{-WSe}_2$  and  $\text{CuWSe}_2$  all four Se atoms are of the same kind (same symmetry) while in  $\text{Cu}_{1/2}\text{WSe}_2$  the two Se atoms are of one kind and the other two of the other kind. We call them Se1 and Se2. As a result of putting one Cu atom in one of the  $2a$  sites, the symmetry changes and the four Se bands split into two groups. This splitting is more prominent in the density of states [Fig. 2(a)].

#### B. Density of states

Figure 2(a) shows the total density of states (DOS) along with the Se  $s$ , Cu  $d$ , and W  $d$  partial DOS for  $\text{Cu}_{1/2}\text{WSe}_2$ . We see that the DOS displays the same four main structures as  $2H\text{-WSe}_2$  (Ref. 11) with the difference that all the peaks are shifted towards the lower energy by  $1\text{--}1.5$  eV with respect to  $E_F$ . The origin of the structures is almost the same in the case of  $2H\text{-WSe}_2$ . The two Se  $s$  states lie between  $-17$  and  $-14$  eV, but the peak of the second Se  $s$  states is shifted towards higher energies by around 0.5 eV with respect to  $E_F$  as shown in Fig. 2(a). As mentioned above, the Se  $s$  states are split into two peaks corresponding to Se1 and Se2. The second structures extending from  $-9$  to  $-1$  eV are composed of W  $d$  and Se  $p$  states along with a significant contribution from the Cu  $d$  states while Cu  $s/p$  has an insignificant contribution. In this region the peak heights are increased over the values of  $2H\text{-WSe}_2$  due to the Cu  $d$  states. The Cu  $d$  states extend from approximately  $2\text{--}4$  eV below  $E_F$ . The Cu  $d$  states in  $\text{Cu}_x\text{WSe}_2$  show the same structure and location with respect to  $E_F$  as in pure copper. We have calculated the number of electrons inside the copper muffin-tin sphere in  $\text{Cu}_x\text{WSe}_2$  and this is same as in the case of pure copper indicating that Cu has a very weak hybridization with the W and Se bands. The third structure extends from  $-0.5$  up to  $5$  eV and the fourth structure extends beyond  $5$  eV. Note that there is no significant change in the third and fourth struc-

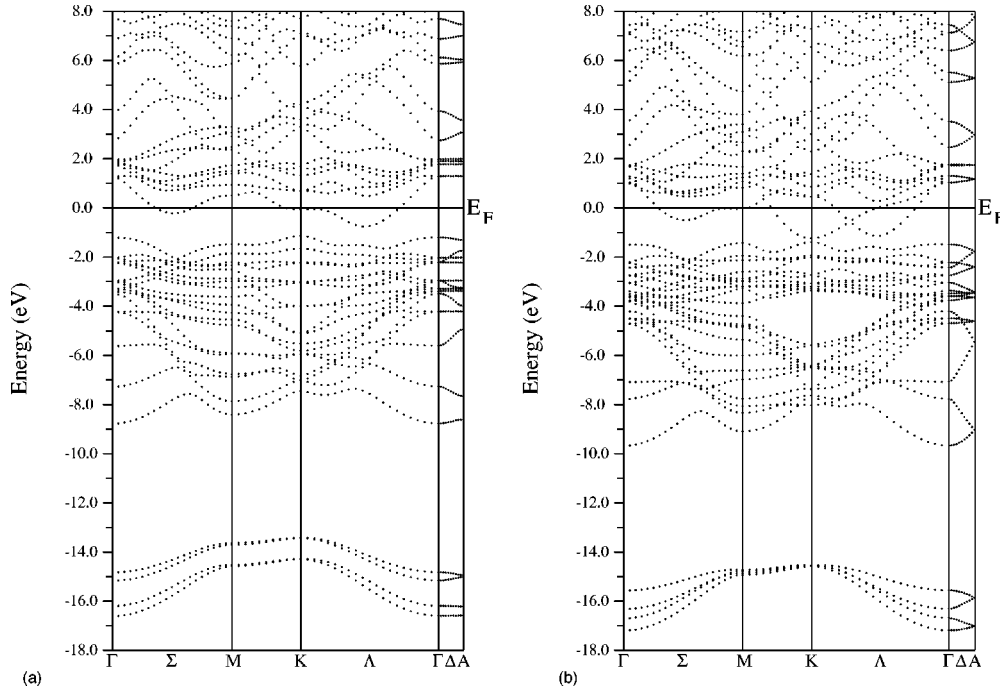


FIG. 1. (a) Band structure of  $\text{Cu}_{1/2}\text{WSe}_2$ . (b) Band structure of  $\text{CuWSe}_2$ .

tures compared to  $2H\text{-WSe}_2$ , except for the shift in the peak position of 1–1.5 eV towards  $E_F$ . Our calculations indicate that  $\text{Cu}_{1/2}\text{WSe}_2$  is metallic. The density of states at  $E_F$ ,  $N(E_F)$ , is about 2.6 (states/eV unit cell).

The total DOS along with the partial Se  $s$ , Cu  $d$ , and W  $d$  for the  $\text{CuWSe}_2$  is shown in Fig. 2(b). The DOS displays four main structures with angular decompositions similar to  $\text{Cu}_{1/2}\text{WSe}_2$ . The first structure (Se  $s$  states) now lies around from  $-17.5$  to  $-14.5$  eV and shows structure similar to  $2H\text{-WSe}_2$ , a band narrowing compared to  $\text{Cu}_{1/2}\text{WSe}_2$  and the peaks shifted towards the lower energy by 1 eV. The second structure from  $-9.5$  to  $-2$  eV is composed of W  $d$  and Se  $p$  states along with a significant contribution from the Cu  $d$  states while Cu  $s/p$  has an insignificant contribution. The density of states at  $E_F$ ,  $N(E_F)$ , is about 4.8 (states/eV unit cell) and is larger than that for  $\text{Cu}_{1/2}\text{WSe}_2$ . This seems to indicate that  $\text{Cu}_x\text{WSe}_2$  is more conducting when  $x$  increases.

#### IV. OPTICAL PROPERTIES

Measurement of the dielectric properties is normally done on single crystals. For compounds having hexagonal or tetragonal symmetry, the experiments are performed with electric vector  $\vec{E}$  parallel or perpendicular to the  $\mathbf{c}$  axis. The corresponding dielectric functions are  $\epsilon^\parallel(\omega)$  and  $\epsilon^\perp(\omega)$ . The calculations of these dielectric function involve the energy eigenvalues and electron wave functions. These are natural outputs of band structure calculations. We have performed calculations of the imaginary part of the interband frequency-dependent dielectric function using the expressions<sup>25</sup>

$$\epsilon_{2\text{inter}}^\parallel(\omega) = \frac{12}{m\omega^2} \int_{\text{BZ}} \sum \frac{|P_{nn'}^Z(k)|^2 dS_k}{\nabla\omega_{nn'}(k)},$$

$$\epsilon_{2\text{inter}}^\perp(\omega) = \frac{6}{m\omega^2} \int_{\text{BZ}} \sum \frac{[|P_{nn'}^X(k)|^2 + |P_{nn'}^Y(k)|^2] dS_k}{\nabla\omega_{nn'}(k)}.$$

The above expressions are written in atomic units with  $e^2 = 1/m = 2$  and  $\hbar = 1$ , where  $\omega$  is the photon energy and  $P_{nn}^X(k)$  is the  $x$  component of the dipolar matrix elements between initial  $|nk\rangle$  and final  $|n'k\rangle$  states with their eigenvalues  $E_n(k)$  and  $E_{n'}(k)$ , respectively.  $\omega_{nn'}(k)$  is the energy difference,

$$\omega_{nn'}(k) = E_n(k) - E_{n'}(k),$$

and  $S_k$  is a constant-energy surface:

$$S_k = \{k; \omega_{nn'}(k) = \omega\}.$$

As the  $\text{Cu}_x\text{WSe}_2$  compounds are metallic, we must include the Drude term (intraband transitions) (Ref. 26)

$$\epsilon_2^\perp(\omega) = \epsilon_{2\text{inter}}^\perp(\omega) + \epsilon_{2\text{intra}}^\perp(\omega),$$

$$\epsilon_{2\text{intra}}^\perp(\omega) = \frac{\omega_p^{\perp 2} \tau}{\omega(1 + \omega^2 \tau^2)},$$

where  $\omega_p$  is the plasma frequency and  $\tau$  is the mean free time between collisions:

$$\omega_p^{\perp 2} = \frac{8\pi}{3} \sum_{kn} \vartheta_{kn}^{\perp 2} \delta(\epsilon_{kn}),$$

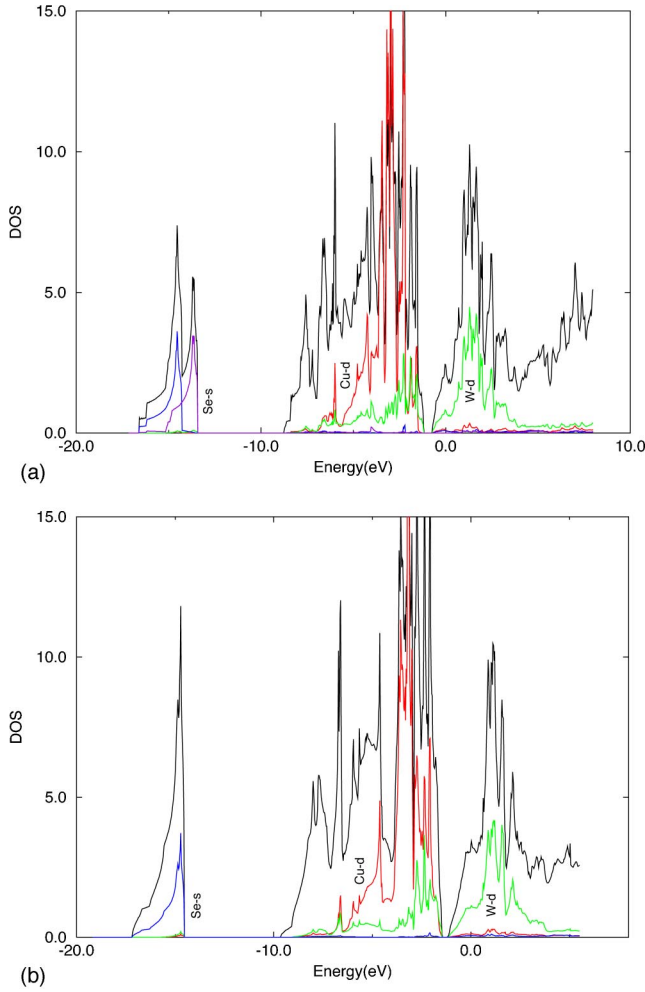


FIG. 2. (a) Total density of states (states/eV unit cell) with the partial, Se1 (light dotted line), Se2 (dark dotted line), Cu  $d$  (dark dashed line), and W  $d$  (light dashed line) DOS for  $\text{Cu}_{1/2}\text{WSe}_2$  (all partial DOS are multiplied by 2). (b) Total density of states (states/eV unit cell) with the partial Se (light dotted line), Cu  $d$  (dark dashed line), and W  $d$  (light dashed line) DOS for  $\text{CuWSe}_2$  (all partial DOS are multiplied by 2).

where  $\varepsilon_{nk}$  is  $E_n(k) - E_F$  and  $\vartheta_{nk}^\perp$  is the electron velocity (in basal plane) squared. Similar expressions for the parallel component can be written. The values of  $\omega_p^\parallel$  and  $\omega_p^\perp$  obtained using the FPLAPW method are given in Table II. The real parts  $\varepsilon_1^\perp(\omega)$  and  $\varepsilon_1^\parallel(\omega)$  can be obtained using the Kramers-Kronig relations.

Figure 3(a) shows  $\varepsilon_2^\perp(\omega)$  and  $\varepsilon_2^\parallel(\omega)$  for  $\text{Cu}_{1/2}\text{WSe}_2$ . We find that  $\varepsilon_2^\perp(\omega)$  and  $\varepsilon_2^\parallel(\omega)$  are anisotropic only at low energies (less than 4 eV). The effect of the Drude (intraband) term is important only at low energies (less than 1 eV). There is one major peak around 1 eV (A) with a major contribution

TABLE II. Plasma frequency in eV.

	$\text{Cu}_{1/2}\text{WSe}_2$	$\text{CuWSe}_2$
$\omega_p^\parallel$	1.53	4.69
$\omega_p^\perp$	3.08	4.54

from  $\varepsilon_2^\parallel(\omega)$ . This structure is not present in  $2H\text{-WSe}_2$  and is attributed to the change in band structure near  $E_F$  as a result of intercalation. In comparison with  $2H\text{-WSe}_2$  we observe that all the other structures are shifted towards lower energies by around 2 eV. The minor peaks are around 3.0 eV (B), 4 eV (C), and 6 eV (D). It would be worthwhile to attempt to identify the transitions that are responsible for the structures in  $\varepsilon_2^\perp(\omega)$  and  $\varepsilon_2^\parallel(\omega)$  using our calculated band structure. The main peak around 1 eV (A) is dominated by transitions from band No. 22 to 23 (from Se  $p$  to W  $d$ ) in the  $\Gamma\Sigma$  and  $MK$  directions, the peak around 3.0 eV (B) is dominated by transitions from band No. 21 to 24 around  $M$ , the peak around 4 eV (C) is dominated by transitions from band No. 19 to 26 and from band No. 20 to 27 in the  $K\Gamma$  direction, and the peak around 6 eV (D) from band No. 18 to 29 and band No. 17 to 30 in the  $MK$  direction.

Figure 3(b) shows  $\varepsilon_2^\perp(\omega)$  and  $\varepsilon_2^\parallel(\omega)$  for  $\text{CuWSe}_2$ .  $\varepsilon_2^\perp(\omega)$  has major contribution in the low-energy range around 1 eV (A). At energies beyond 3 eV (B) both polarizations contribute. We observe that at low energy  $\varepsilon_1^\perp(\omega)$  is extremely large. The peak around 1.5 eV (A) is dominated by transitions from band No. 24 to 25 in the  $\Gamma M$  direction. The peak around 1.5

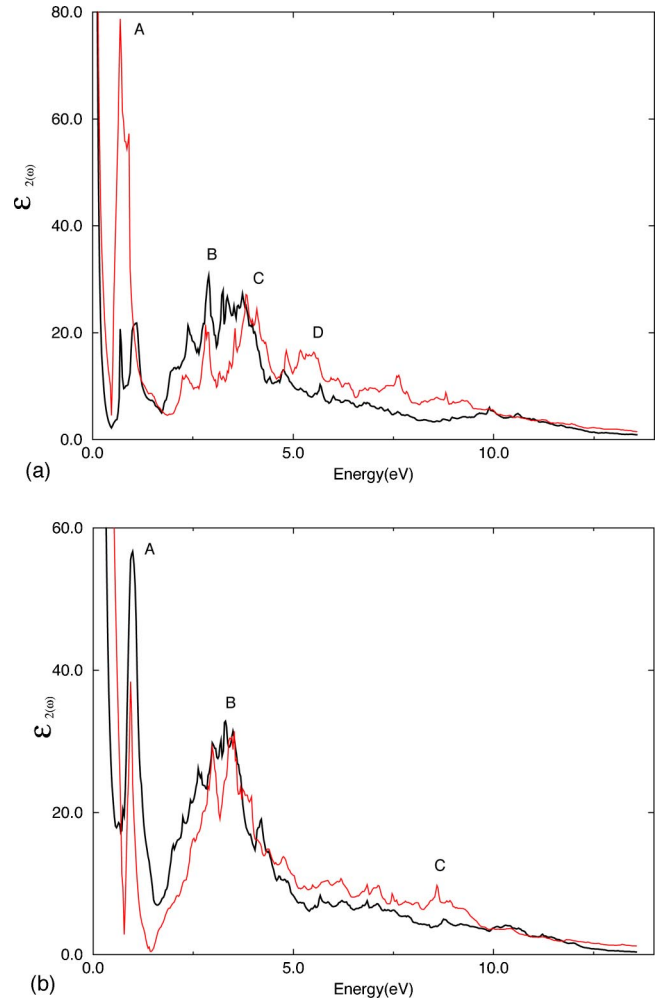


FIG. 3. (a) Calculated  $\varepsilon_2^\perp(\omega)$  (light line) and  $\varepsilon_2^\parallel(\omega)$  (dark line) for  $\text{Cu}_{1/2}\text{WSe}_2$ . (b) Calculated  $\varepsilon_2^\perp(\omega)$  (light line) and  $\varepsilon_2^\parallel(\omega)$  (dark line) for  $\text{CuWSe}_2$ .

eV (*A*) is dominated by transition from band No. 24 to 26 around *K*, and the peak at 3.5 eV (*B*) is dominated by transitions from band No. 23 to 27 and band No. 22 to 26 in the *MK* direction. The higher-energy peaks seem to become less distinct, almost merging with the background.

## V. CONCLUSION

We have studied the electronic and optical properties of  $\text{Cu}_x\text{WSe}_2$  for ( $x=0.5$  and 1). When intercalating with copper ( $x=0.5$ ) we find that the conduction and valence bands are shifted towards lower energies by 1–1.5 eV with respect to  $E_F$  in comparison with *2H*-WSe<sub>2</sub> and this closes the gap at  $E_F$ , which indicates that  $\text{Cu}_{1/2}\text{WSe}_2$  is metallic. The DOS at  $E_F$ ,  $N(E_F)$ , is about 2.6 (states/eV unit cell). There is a splitting of the Se *s* structure into two peaks due to symmetry breaking. When intercalating with more copper ( $x=1$ ) there is a further shifting of the conduction and valence bands towards the lower energies by 1 eV with respect to  $E_F$  in comparison with  $\text{Cu}_{1/2}\text{WSe}_2$ . The DOS of  $E_F$ ,  $N(E_F)$ , is about 4.8 (states/eV unit cell). This seems to indicate that  $\text{CuWSe}_2$  is more conducting than  $\text{Cu}_{1/2}\text{WSe}_2$ , in agreement with the experimental work of Patel *et al.*<sup>20</sup> Our analysis of partial DOS indicates that Cu *d* bands are very flat and con-

tribute significantly to the DOS in the range 2–4 eV below  $E_F$ , in the Cu-intercalated *2H*-WSe<sub>2</sub> compounds. The Cu partial DOS in  $\text{Cu}_x\text{WSe}_2$  compounds is similar to the partial DOS of pure copper in terms of bandwidth and location with respect to  $E_F$ . We find that Cu hybridizes weakly with the W and Se states.

Our calculations of the optical properties shows that there is a considerable anisotropy between  $\epsilon^\perp(\omega)$  and  $\epsilon^\parallel(\omega)$  for  $\text{Cu}_x\text{WSe}_2$ . The  $\epsilon^\perp(\omega)$  and  $\epsilon^\parallel(\omega)$  for  $\text{Cu}_{1/2}\text{WSe}_2$  is different from that of *2H*-WSe<sub>2</sub> in terms of peak heights and peak locations. There is one large enhanced peak at around 1 eV, while the other peaks are similar to those of *2H*-WSe<sub>2</sub>. In  $\text{CuWSe}_2$  the low-energy peak is shifted to lower energies and is much larger than the low-energy peak of  $\text{Cu}_{1/2}\text{WSe}_2$  while the large energy peaks merge with the background. There is no experimental optical data for  $\text{Cu}_{1/2}\text{WSe}_2$  and  $\text{CuWSe}_2$ .

## ACKNOWLEDGMENT

We would like to thank the Institute Computer Center and Physics Department for providing the computational facilities.

- 
- <sup>1</sup>E. Bucher, in *Photoelectrochemistry and Photovoltaics of Layered Semiconductors*, edited by A. Aruchamy (Kluwer Academic, Dordrecht, 1992), p. 1.
- <sup>2</sup>G. V. Subbarao and C. S. Sunandana, *Preparation and Characterisation of Materials* (Academic, London, 1989), p. 269.
- <sup>3</sup>J. Pouzet and J. C. Berned, *Diffus. Defect Data*, Pt. B **37–38**, 485 (1994).
- <sup>4</sup>G. Prasad and O. N. Srivastava, *J. Phys. D* **21**, 1028 (1988).
- <sup>5</sup>G. H. Yousefi, *Mater. Lett.* **9**, 38 (1989).
- <sup>6</sup>R. Knoenkamp, *Phys. Rev. B* **38**, 3056 (1988).
- <sup>7</sup>R. Coehoorn *et al.*, *Phys. Rev. B* **35**, 6195 (1987).
- <sup>8</sup>Th. Straub *et al.*, *Phys. Rev. B* **53**, R16 152 (1996).
- <sup>9</sup>Th. Finteis *et al.*, *Phys. Rev. B* **55**, 10 400 (1997); **59**, 2461(E) (1999).
- <sup>10</sup>M. Traving *et al.*, *Phys. Rev. B* **55**, 10 392 (1997).
- <sup>11</sup>S. Sharma *et al.*, *Phys. Rev. B* **60**, 8610 (1999).
- <sup>12</sup>A. R. Beal, J. C. Knights, and W. Y. Liang, *J. Phys. C* **5**, 3540 (1972).
- <sup>13</sup>W. Y. Liang, *J. Phys. C* **6**, 551 (1973).
- <sup>14</sup>A. R. Beal, W. Y. Liang, and H. P. Hughes, *J. Phys. C* **9**, 2449 (1976).
- <sup>15</sup>K. K. Kam, C. L. Chang, and D. W. Lynch, *J. Phys. C* **17**, 9031 (1984).
- <sup>16</sup>T. Kusawake, Y. Takahashi, and K. Ohshima, *J. Phys.: Condens. Matter* **11**, 6121 (1999).
- <sup>17</sup>T. Kusawake *et al.*, *J. Phys.: Condens. Matter* **13**, 9913 (2001).
- <sup>18</sup>T. Kusawake, Y. Takahashi, and K. Ohshima, *Mater. Res. Bull.* **33**, 1009 (1998).
- <sup>19</sup>A. Klein *et al.*, *Surf. Sci.* **321**, 19 (1994).
- <sup>20</sup>J. B. Patel *et al.*, (unpublished).
- <sup>21</sup>P. Blaha, K. Schwarz, and J. Luitz, computer code WIEN97, Vienna University of Technology, 1997 (improved and updated unix version of the original copyright WIEN Code) which was published by P. Blaha *et al.*, *Comput. Phys. Commun.* **59**, 399 (1990).
- <sup>22</sup>O. Jepsen and O. K. Andersen, *Solid State Commun.* **9**, 1763 (1971); G. Lehmann and M. Taut, *Phys. Status Solidi B* **54**, 496 (1972).
- <sup>23</sup>J. A. Wilson and A. D. Yoffe, *Adv. Phys.* **18**, 193 (1969).
- <sup>24</sup>C. Ambrosch-Draxl *et al.*, *Phys. Rev. B* **51**, 9668 (1995).
- <sup>25</sup>Sangeeta Sharma, S. Auluck, and M. A. Khan, *Pramana, J. Phys.* **54**, 431 (2000).
- <sup>26</sup>F. Wooten, *Optical Properties of Solids* (Academic, New York, 1972).